

Matter-antimatter asymmetry without loops

Arnab Dasgupta¹, P. S. Bhupal Dev², Yongchao Zhang^{2,3}

¹*School of Liberal Arts, Seoul-Tech, Seoul 139-743, Korea*

²*Department of Physics and McDonnell Center for the Space Sciences,
Washington University, St. Louis, MO 63130, USA and*

³*Department of Physics, Oklahoma State University, Stillwater, OK 74078, USA*

We propose a new mechanism for generating matter-antimatter asymmetry via the interference of tree-level diagrams only. We first derive a general result that a nonzero CP -asymmetry can be generated via at least two sets of interfering tree-level diagrams involving either $2 \rightarrow 2$ or $1 \rightarrow \mathcal{N}$ (with $\mathcal{N} \geq 3$) processes. We illustrate this point in a simple TeV-scale extension of the Standard Model with an inert Higgs doublet and right-handed neutrinos, along with an electroweak-triplet scalar field. The imaginary part needed for the required CP -asymmetry comes from the trilinear coupling of the inert-doublet with the triplet scalar. Small Majorana neutrino masses are generated by both scotogenic and type-II seesaw mechanisms. The real part of the neutral component of the inert-doublet serves as a cold dark matter candidate. The evolutions of the dark matter relic density and the baryon asymmetry are intimately related in this scenario.

Introduction.— The observed asymmetry between the number densities of baryonic matter and antimatter in the universe [1] cannot be accounted for in the Standard Model (SM). Therefore, a viable baryogenesis mechanism is an essential ingredient for the success of any beyond SM physics scenario. The dynamical generation of baryon asymmetry requires three basic Sakharov conditions [2] to be satisfied: (i) baryon number violation, (ii) C and CP violation, and (iii) out-of-equilibrium dynamics. A well-known mechanism that satisfies these conditions is the out-of-equilibrium and CP violating $1 \rightarrow 2$ decays of a heavy particle, such as in GUT baryogenesis [3, 4] or leptogenesis [5] (for reviews, see e.g. Refs. [6, 7]). To obtain a baryon/lepton asymmetry in the out-of-equilibrium baryon/lepton number violating $1 \rightarrow 2$ decays of heavy particles, one must consider the interference between tree-level diagrams and higher-order loop diagrams. Furthermore, some particles in the loop must be able to go on-shell, and the interaction between the intermediate on-shell particles and the final particles should correspond to a net change in baryon/lepton number for the net asymmetry to be nonzero [8] (see also Refs. [9, 10]). Similar interference effects between tree and loop-level diagrams have also been considered for generating the baryon asymmetry from $2 \rightarrow 2$ scattering [11–14] or annihilation [15–19] processes.

In this *letter*, we argue that the interference between tree and loop diagrams is not the only way to generate a nonzero asymmetry from out-of-equilibrium heavy particle decays/annihilations. We propose a new mechanism where it suffices to consider two sets of interfering diagrams at the tree-level only. The simplest solution is through the tree-level $2 \rightarrow 2$ scattering or $1 \rightarrow \mathcal{N}$ (with $\mathcal{N} \geq 3$) decay processes. In the next section, we discuss the general framework in which this can be realized. Then we will consider a simple $2 \rightarrow 2$ scattering model for leptogenesis to illustrate our main point.

Asymmetry generation without loops.— We claim

that a net lepton or baryon number asymmetry can be generated from the interference effect of two sets of tree-level decay or scattering diagrams with the same initial and final states, as long as the following two conditions are satisfied:

- (i) There is a net nonzero lepton or baryon number between the initial and final states.¹
- (ii) At least one set of the decay or scattering amplitudes is complex such that the squared amplitudes for particles and antiparticles are different, giving rise to a net CP -asymmetry.

The simplest way to achieve this is through $2 \rightarrow 2$ scatterings (or $1 \rightarrow 3$ decays) involving two *different* intermediate-state particles, with the outgoing particles (or decay products) carrying a net nonzero baryon or lepton number. Without loss of generality, we focus on the simplest $2 \rightarrow 2$ scattering case with the initial states i_1, i_2 and with only two subprocesses for the final states f_1, f_2 (here $i_{1,2}$ and $f_{1,2}$ generically stand for bosons and/or fermions), mediated by intermediate-state particles of mass m_1 and m_2 , respectively; see Fig. 1. The total amplitude for the final state *particles* $f_1 f_2$ is

$$\mathcal{M} = \mathcal{C}_1 \mathcal{M}_1 + \mathcal{C}_2 \mathcal{M}_2, \quad (1)$$

where \mathcal{C}_i contains only the couplings and \mathcal{M}_i is the rest of the amplitude. The corresponding amplitude for the *anti-particles* $\bar{f}_1 \bar{f}_2$ (with the same initial state $i_1 i_2$) is

$$\bar{\mathcal{M}} = \mathcal{C}_1^* \mathcal{M}_1 + \mathcal{C}_2^* \mathcal{M}_2. \quad (2)$$

Comparing the modular square of the amplitudes, we obtain the CP asymmetry factor

$$\delta = |\mathcal{M}|^2 - |\bar{\mathcal{M}}|^2 = -4 \text{Im}[\mathcal{C}_1 \mathcal{C}_2^*] \text{Im}[\mathcal{M}_1 \mathcal{M}_2^*], \quad (3)$$

¹ In principle, this condition can be somewhat relaxed if we consider flavor-dependent asymmetries, with zero net lepton or baryon number in the final state, as in flavored leptogenesis (for recent reviews, see Refs. [20, 21]). For simplicity, here we will not consider such flavor-dependent effects.

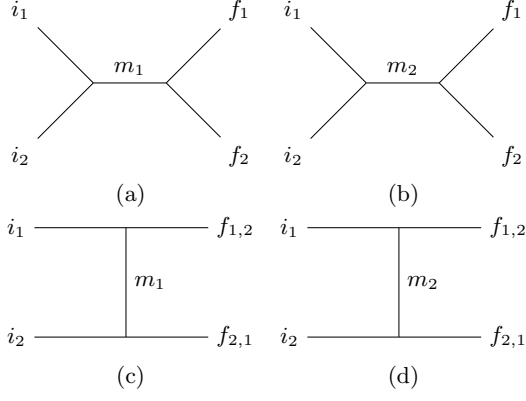


FIG. 1. Generic topologies for tree-level $2 \rightarrow 2$ subprocesses that can give rise to nonzero lepton or baryon asymmetry. Here $i_{1,2}$ and $f_{1,2}$ are respectively the initial and final states, and $m_{1,2}$ are the masses of two different mediators.

where $\text{Im}[\mathcal{C}_1\mathcal{C}_2^*]$ is the imaginary part coming from the couplings, which is required to be nonzero for CP violation, and $\text{Im}[\mathcal{M}_1\mathcal{M}_2^*]$ incorporates the imaginary part from the sub-amplitudes $\mathcal{M}_{1,2}$, which is reminiscent of the imaginary part coming from the interference of tree and loop diagrams in the $1 \rightarrow 2$ decay scenario. Note that for $1 \rightarrow 2$ decays, the tree-level decay rates for $f_1 f_2$ and $\bar{f}_1 \bar{f}_2$ final states are both proportional to the modular square of the same coupling, which implies $\delta = 0$. Eq. (3) is a general result applicable to $2 \rightarrow 2$ scatterings, as well as $1 \rightarrow \mathcal{N}$ decays (for $\mathcal{N} \geq 3$).

In the tree-level $2 \rightarrow 2$ processes shown in Fig. 1, we have only one source for the complex sub-amplitudes, which is due to the finite widths of the mediators.² In general, the sub-amplitudes $\mathcal{M}_{1,2}$ can be written as

$$\mathcal{M}_j = \frac{A_j}{x_j - m_j^2 + im_j\Gamma_j}, \quad (4)$$

with $j = 1, 2$, $x_j = s, t, u$ the Mandelstam variables, m_j and Γ_j respectively the mediator masses and widths, and A_j some arbitrary real parameters. The imaginary component of the product of amplitudes appearing in Eq. (3) can then be written as

$$\text{Im}[\mathcal{M}_1\mathcal{M}_2^*] = \frac{A_1 A_2 [(x_1 - m_1^2)m_2\Gamma_2 - (x_2 - m_2^2)m_1\Gamma_1]}{[(x_1 - m_1^2)^2 + m_1^2\Gamma_1^2][(x_2 - m_2^2)^2 + m_2^2\Gamma_2^2]}, \quad (5)$$

which is non-vanishing as long as $(x_1 - m_1^2)m_2\Gamma_2 \neq (x_2 - m_2^2)m_1\Gamma_1$. With the imaginary part of the couplings

$\text{Im}[\mathcal{C}_1\mathcal{C}_2^*] \neq 0$, we can then produce a nonzero asymmetry [cf. Eq. (3)]. This general argument holds, irrespective of the specific subprocesses or the model details.

For the tree-level topologies shown in Fig. 1, we can have three distinct possibilities for the two subprocesses to realize $\text{Im}[\mathcal{M}_1\mathcal{M}_2^*] \neq 0$ in Eq. (5):

i) If both subprocesses are in the s -channel [cf. Fig. 1 (a)+(b)], one just needs to replace $x_{1,2}$ by s in Eq. (5). In this case, the CP -asymmetry factor δ in Eq. (3) can be largely enhanced in the vicinity of the resonance(s), with $s - m_i^2 \simeq m_i\Gamma_i$ (with $i = 1, 2$), similar to the enhancement effect in resonant leptogenesis [24, 25].

ii) If one of the sub-amplitudes is in the s -channel and the other one in the t - or u -channel [cf. Fig. 1 (a)+(d) or (b)+(c)], one can safely neglect the imaginary part for the t - or u -channel propagator. For concreteness, we take \mathcal{M}_1 as the s -channel and \mathcal{M}_2 as the x -channel ($x = t$ or u) amplitude. In this case, Eq. (5) is simplified to

$$\text{Im}[\mathcal{M}_1\mathcal{M}_2^*] \simeq -\frac{A_1 A_2 m_1 \Gamma_1}{[(s - m_1^2)^2 + m_1^2 \Gamma_1^2](x - m_2^2)}, \quad (6)$$

which is proportional to the s -channel mediator width Γ_1 . Here also the CP -asymmetry could be largely enhanced at the s -channel resonance, i.e. $s - m_1^2 \simeq m_1\Gamma_1$.

iii) If both subprocesses are in the t - or u -channel [cf. Fig. 1 (c)+(d)], then the width terms in the denominator of Eq. (5) can be neglected, i.e.

$$\text{Im}[\mathcal{M}_1\mathcal{M}_2^*] \simeq \frac{A_1 A_2 [(x_1 - m_1^2)m_2\Gamma_2 - (x_2 - m_2^2)m_1\Gamma_1]}{(x_1 - m_1^2)^2(x_2 - m_2^2)^2}. \quad (7)$$

As a result, the CP -asymmetry is suppressed by the ratio $m_i\Gamma_i/(x_j - m_j^2)$ with $i, j = 1, 2$.

In what follows, we will consider a concrete model realization for the case *ii)* and illustrate the baryon asymmetry generation with a few benchmark points (BPs).

The model.— To illustrate our tree-level mechanism in a minimal realistic extension of the SM, we consider an amalgamation of the scotogenic model [26] and type-II seesaw [27–31]. For the purpose of scotogenic mechanism, an inert $SU(2)_L$ -doublet scalar $\eta \equiv (\eta^+, \eta^0)$ and three right-handed neutrinos (RHNs) N_i (with $i = 1, 2, 3$) are introduced. To implement type-II seesaw, an $SU(2)_L$ -triplet scalar $\Delta \equiv (\Delta^{++}, \Delta^+, \Delta^0)$ is added. The inert doublet η and the three RHNs N_i are odd under a discrete Z_2 symmetry, while all other particles are even. In this model, we assume the RHNs are heavier than the η scalars, thus the lightest neutral component η^0 plays the role of dark matter [26]. A nonminimal coupling of the inert doublet gravity can also successfully accommodate inflation [32].

The relevant Yukawa couplings are given by the Lagrangian

$$-\mathcal{L}_Y = Y_{i\alpha}^N \bar{\eta}^\dagger L_\alpha N_i + Y_{\alpha\beta}^\Delta \bar{L}_\alpha^\dagger \Delta L_\beta + \text{H.c.}, \quad (8)$$

² One may argue that the finite width is also a loop-induced effect for unstable particle decays, since it is related to the imaginary part of the self-energy [22, 23]. However, the crux of our discussion is that we only require a nonzero width, whereas the $1 \rightarrow 2$ decay case needs both nonzero width and interference between tree and loop (self-energy and/or vertex correction) diagrams.

with $L \equiv (\nu, \ell)$ being the SM lepton doublet, C the charge conjugation operator, $\tilde{\eta} = i\sigma_2\eta^*$ (σ_2 being the second Pauli matrix), $\alpha, \beta = e, \mu, \tau$ the lepton flavor indices, and $i = 1, 2, 3$ the RHN indices. For simplicity, we assume there is no mixing nor CP phase in the RHN sector. The most general scalar potential for the SM Higgs doublet $H \equiv (H^+, H^0)$, inert doublet η and triplet Δ is given by

$$\begin{aligned} V \supset & -\mu_H^2(H^\dagger H) + \mu_\eta^2(\eta^\dagger \eta) - \mu_\Delta^2 \text{Tr}[\Delta^\dagger \Delta] \\ & + (\mu_{H\Delta}\tilde{H}^\dagger \Delta H + \mu_{\eta\Delta}\eta^\dagger \Delta^\dagger \tilde{\eta} + \text{H.c.}) \\ & + \lambda_H(H^\dagger H)^2 + \lambda_\eta(\eta^\dagger \eta)^2 + \lambda_\Delta\{\text{Tr}[\Delta^\dagger \Delta]\}^2 \\ & + \lambda'_\Delta \text{Tr}[\Delta^\dagger \Delta \Delta^\dagger \Delta] + \lambda_{H\eta}|H^\dagger \eta|^2 + \lambda'_{H\eta}(H^\dagger H)(\eta^\dagger \eta) \\ & + \lambda''_{H\eta}((H^\dagger \eta)^2 + \text{H.c.}) + \lambda_{H\Delta}(H^\dagger H)\text{Tr}[\Delta^\dagger \Delta] \\ & + \lambda'_{H\Delta}\text{Tr}[H^\dagger \Delta \Delta^\dagger H] + \lambda_{\eta\Delta}(\eta^\dagger \eta)\text{Tr}[\Delta^\dagger \Delta] \\ & + \lambda'_{\eta\Delta}\text{Tr}[\eta^\dagger \Delta \Delta^\dagger \eta], \end{aligned} \quad (9)$$

where $\tilde{H} = i\sigma_2 H^*$ and the mass parameters $\mu_{H,\eta,\Delta}^2 > 0$ so that both H and Δ obtain non-vanishing vacuum expectation values (VEVs), i.e. $\langle H^0 \rangle = v \simeq 246$ GeV and $\langle \Delta^0 \rangle = v_\Delta$. The mass parameter $\mu_{\eta\Delta}$ is chosen to be complex, which is crucial for the CP -asymmetry [cf. Eq. (3)]. All other parameters in Eq. (9) are assumed to be real. The physical masses for the neutral and charged scalars can be obtained from the minimization of the potential (9), which is detailed in the Appendix. Note that here the doublet η is odd under the Z_2 symmetry and does not mix the SM Higgs and the triplet, which is necessary for the neutral real component η_R to be a stable DM candidate.

In this setup the neutrino mass is generated from both loop-level scotogenic and tree-level type-II seesaw mechanisms, which are induced respectively by the Yukawa couplings Y^N and Y^Δ given in Eq. (8):

$$m_\nu = (Y^N)^\top \Lambda Y^N + Y^\Delta v_\Delta, \quad (10)$$

where Λ is an effective loop-suppressed RHN mass scale, given by [26, 33]

$$\begin{aligned} \Lambda_{ii} = & \frac{m_{N_i}}{16\pi^2} \left[\frac{m_{\eta_R}^2}{m_{N_i}^2 - m_{\eta_R}^2} \ln \left(\frac{m_{N_i}^2}{m_{\eta_R}^2} \right) \right. \\ & \left. - \frac{m_{\eta_I}^2}{m_{N_i}^2 - m_{\eta_I}^2} \ln \left(\frac{m_{N_i}^2}{m_{\eta_I}^2} \right) \right]. \end{aligned} \quad (11)$$

We have assumed the RHNs do not mix with each other, therefore Λ is a diagonal matrix. The Yukawa couplings in Eq. (10) are related to the neutrino oscillation data, Λ and v_Δ as follows:

$$Y_{i\alpha}^N = F_I^{1/2} \left(\Lambda^{-1/2} \mathcal{O} \hat{m}_\nu^{1/2} U_{\text{PMNS}}^\dagger \right)_{i\alpha}, \quad (12)$$

$$Y_{\alpha\beta}^\Delta = F_{\text{II}} v_\Delta^{-1} (U_{\text{PMNS}}^* \hat{m}_\nu U_{\text{PMNS}}^\dagger)_{\alpha\beta}, \quad (13)$$

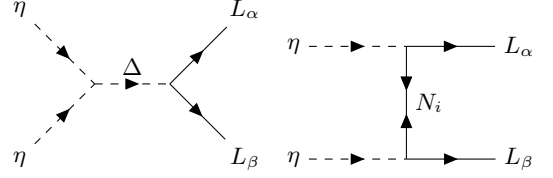


FIG. 2. Feynman diagrams for the $2 \rightarrow 2$ scattering processes $\eta\eta \rightarrow LL$ in our example model.

where $\hat{m}_\nu = \{m_{\nu_1}, m_{\nu_2}, m_{\nu_3}\}$ the diagonal neutrino mass eigenvalues, and U_{PMNS} the PMNS lepton mixing matrix. In Eq. (12) we have used the Casas-Ibarra parametrization [34] for the coupling Y^N , with \mathcal{O} an arbitrary orthogonal matrix. F_I and F_{II} are the fractions of contributions to neutrino mass matrix from the radiative scotogenic and tree-level type-II seesaw mechanisms respectively, with $F_I + F_{\text{II}} = 1$.

Boltzmann equations.— As stated above, the matter asymmetry is generated from the interference effects between two tree-level diagrams, which are shown in Fig. 2 for our scotogenic type-II seesaw model. In particular, we analyze the $2 \rightarrow 2$ $\Delta L = 2$ scattering processes

$$\eta\eta \rightarrow L_\alpha L_\beta, \quad (14)$$

which include $\eta^\pm \eta^\pm \rightarrow \ell_\alpha \ell_\beta$, $\eta^0 \eta^\pm \rightarrow \ell_\alpha \nu_\beta$ and $\eta^0 \eta^0 \rightarrow \nu_\alpha \nu_\beta$. These processes can be mediated by an s -channel triplet scalar Δ , and also by RHNs N_i in the t - and u -channels, as shown in Fig. 2. The effective CP -asymmetry factor [cf. Eq. (3)] is given by

$$\begin{aligned} \delta = & \sum_{\alpha\beta} 4 \text{Im} \left[\mu_{\eta\Delta} Y_{i\alpha}^N Y_{\alpha\beta}^{\Delta*} Y_{i\beta}^N \right] \\ & \times \frac{sm_{N_i} m_\Delta \Gamma_\Delta}{(s - m_\Delta^2)^2 + m_\Delta^2 \Gamma_\Delta^2} \left[\frac{1}{t - m_{N_i}^2} + \frac{1}{u - m_{N_i}^2} \right], \end{aligned} \quad (15)$$

where Γ_Δ is the triplet scalar width. Here the imaginary part comes purely from the combinations of the Yukawa couplings Y^N , Y^Δ [cf. Eq. (8)] and the trilinear coupling $\mu_{\eta\Delta}$ [cf. Eq. (9)], which can be parametrized as

$$\begin{aligned} & \sum_{\alpha\beta} \text{Im} \left[\mu_{\eta\Delta} Y_{i\alpha}^N Y_{\alpha\beta}^{\Delta*} Y_{i\beta}^N \right] \\ & = F_I F_{\text{II}} v_\Delta^{-1} \text{Im} \left\{ \mu_{\eta\Delta} \text{Tr} \left[\Lambda^{-1/2} \mathcal{O} \hat{m}_\nu^2 \mathcal{O}^\top \Lambda^{-1/2} \right] \right\}. \end{aligned} \quad (16)$$

In general the \mathcal{O} matrix might also be complex, thus contributing to the imaginary part in Eq. (16).

It is interesting that part of the same $2 \rightarrow 2$ process (14) containing η^0 also contributes to the (co)annihilation of DM particles. In this sense, the time evolutions of the DM relic density and the lepton asymmetry are related, as we will see below. The freeze-out mechanism for the DM is identical to the standard inert-doublet case [36, 37], where we can have $\eta\eta \rightarrow \text{SM SM}$

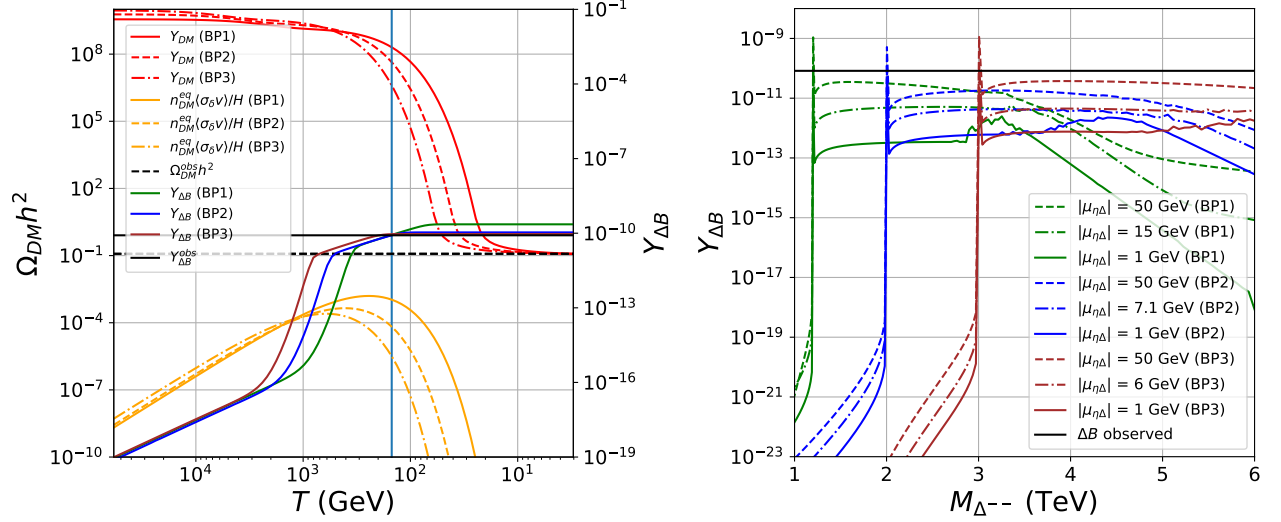


FIG. 3. *Left*: Net baryon number density $Y_{\Delta B}$, DM density Y_{DM} and $n_{DM}^{eq} \langle \sigma v \rangle_{\delta} / H$ as functions of temperature T , for the three benchmark points given in Table I. *Right*: Net baryon number density $Y_{\Delta B}$ as function of the Δ -mediator mass, for three different values of $|\mu_{\eta\Delta}|$ (with the argument of $\pi/2$) for each of the three benchmark points in Table I. The solid horizontal black line (on both panels) indicates the observed baryon number density $Y_{\Delta B}^{obs} = (8.718 \pm 0.004) \times 10^{-11}$, and the dashed horizontal black line (on the left panel) indicates the observed DM relic density $\Omega_{DM}^{obs} h^2 = 0.120 \pm 0.001$ [1]. The vertical solid line (on the left panel) represents the sphaleron freeze-out temperature $T_{sph} = 131.7 \pm 2.3$ GeV [35].

with ‘SM’ standing for all SM fermions (quarks and leptons), gauge bosons W, Z and Higgs boson h .

The genesis of DM relic density and leptonic asymmetry are both governed by the coupled Boltzmann equations

$$\frac{dY_{\eta}}{dz} = \frac{-s}{H(z)z} [(Y_{\eta}^2 - (Y_{\eta}^{eq})^2) \langle \sigma v \rangle (\eta\eta \rightarrow \text{SM SM})], \quad (17)$$

$$\begin{aligned} \frac{dY_{\Delta L}}{dz} = & \frac{s}{H(z)z} [(Y_{\eta}^2 - (Y_{\eta}^{eq})^2) \langle \sigma v \rangle_{\delta} (\eta\eta \rightarrow LL) \\ & - 2Y_{\Delta L} Y_{\ell}^{eq} r_{\eta}^2 \langle \sigma v \rangle_{\text{tot}} (\eta\eta \rightarrow LL) \\ & - 2Y_{\Delta L} Y_{\eta}^{eq} \langle \sigma v \rangle (\eta \bar{L} \rightarrow \eta L)] , \end{aligned} \quad (18)$$

where $z = m_{\eta}/T$, $Y_i^{(eq)} \equiv n_i^{(eq)}/s$ are the normalized number densities (in equilibrium) for the particles i (s being the entropy density), $Y_{\Delta L} = Y_L - Y_{\bar{L}}$, $r_{\eta} = Y_{\eta}^{eq}/Y_{\ell}^{eq}$, and $H(z) = \sqrt{8\pi^3 g_*/90} m_{\eta}^2/(z^2 M_{Pl})$ with M_{Pl} the Planck scale and g_* the number of relativistic degrees of freedom at temperature T . Here $\langle \sigma v \rangle$ are the thermally-averaged annihilation/scattering rates: $\langle \sigma v \rangle (\eta\eta \rightarrow \text{SM SM})$ is the DM annihilation rate, $\langle \sigma v \rangle_{\text{tot}} (\eta\eta \rightarrow LL)$ is the thermally-averaged scattering cross section for $\eta\eta \rightarrow LL$ that includes also the $\Delta L = 0$ processes such as $\eta^+ \eta^- \rightarrow \ell^+ \ell^-$, whereas $\langle \sigma v \rangle_{\delta} (\eta\eta \rightarrow LL)$ only includes the $\Delta L = 2$ processes listed below Eq. (14). The expressions for all thermal cross sections in Eq. (18) are collected in the Appendix. Evaluating the Boltzmann equations above, one can obtain the lepton asymmetry $Y_{\Delta L}(z)$, which is then converted to baryon asymmetry $Y_{\Delta B} = -(28/51)Y_{\Delta L}$ [38]

via the standard electroweak sphaleron processes [39] at the sphaleron transition temperature T_{sph} . In an analogous way, one can also calculate the evolution of the DM density Y_{η} from Eq. (17) and get the final relic abundance $\Omega_{DM} h^2 = 2.755 \times 10^8 Y_{\eta}(m_{\eta}/\text{GeV})$ at DM freeze-out temperature $T_f \simeq m_{\eta}/20$.

Numerical results.— We solve the Boltzmann equations (17) and (18) numerically for three representative benchmark points (BP1, BP2, BP3) given in Table I in the Appendix, obtained by implementing our model in SARAH 4 [40] and after checking consistency with all existing experimental constraints. We assume $F_I = F_{II} = 1/2$ in Eqs. (12) and (13), i.e. equal contributions from scotogenic and tree-level type-II seesaw to neutrino masses. This choice maximizes the CP -asymmetry in Eq. (16), subject to keeping other factors the same. In addition, the \mathcal{O} matrix is taken to be identity, so that $\mathcal{O} \hat{m}_{\nu}^2 \mathcal{O}^T = \hat{m}_{\nu}^2$, and the mass parameter $\mu_{\eta\Delta}$ is assumed to be purely imaginary in Eq. (16). The RHNs are taken to be much heavier than the η particles to avoid the wash-out of lepton asymmetry from the inverse decay processes $L\eta \rightarrow N_i$. For the benchmark points we take, the mass splitting $m_{\eta_I} - m_{\eta_R}$ is larger than 100 keV scale, such that the direct detection constraints for inelastic scattering of DM with nucleons [41–43] can be evaded.

The evolutions of the DM relic density $\Omega_{DM} h^2$ and the baryon asymmetry $Y_{\Delta B}$ are evaluated using micrOMEGAS 5.0 [44] and the results are presented in Fig. 3. In the left panel of Fig. 3, we have shown the time evolution of the DM relic density by red solid, dashed and dot-dashed curves for BP1, BP2, and BP3 respectively. The

observed value of the relic density is obtained in each case by fixing the Higgs-DM quartic couplings $\lambda'_{\eta H} = -\lambda''_{\eta H} = \lambda_{\eta H}$ in Eq. (9) for a given mass scale (μ_η) as shown in Table I. The magnitude of the required Higgs-DM quartic coupling increases with the DM mass as the effective freeze-out cross-section goes as $\langle\sigma v\rangle \sim \lambda_{H\eta}^2/m_\eta^2$.

For each choice of the DM mass, the maximal contribution to the baryon asymmetry comes in the vicinity of the s -channel resonance in Fig. 2 i.e when $2m_\eta \rightarrow m_\Delta$. So in the left panel of Fig. 3, we have fixed the Δ -mediator mass at the resonance point and have satisfied the required baryon asymmetry by appropriately fixing the trilinear coupling $\mu_{\eta\Delta}$ as shown in Table I. We find that the size of the trilinear coupling needed for the asymmetry decreases as the mass of the DM increases.

The effect of the trilinear coupling $\mu_{\eta\Delta}$ and of the mediator mass on the baryon asymmetry is further illustrated in the right panel of Fig. 3. For each of the three BPs given in Table I, we show the variation of $Y_{\Delta B}$ as a function of the mediator mass for different values of $\mu_{\eta\Delta}$ (as shown by the solid, dashed and dot-dashed lines with green, blue and red corresponding to BP1, BP2, and BP3, respectively). The enhancement of the asymmetry at the resonance point where $m_\Delta = 2m_\eta$ can be clearly seen. Also, increasing the size of the trilinear coupling results in a larger asymmetry, as expected. We have fixed the trilinear coupling for each BP in Table I to be the minimum value for which the observed baryon asymmetry can be obtained at the resonance. Note that for larger trilinear couplings, one can also achieve the observed asymmetry away from the resonance point.

Collider signals.— The BPs chosen for our model to simultaneously explain baryogenesis, dark matter and neutrino mass involve TeV-scale beyond SM scalars and heavy RHNs which can be directly tested at current and future high-energy colliders. For instance, the neutral and charged triplet scalars can be directly searched for at the LHC [45, 46], as well as in future HL-LHC [47–51], 100 TeV hadron colliders [50, 52] and lepton colliders [53], or indirectly probed in the high-precision low-energy experiments like MOLLER [54]. The charged η^\pm scalars can be produced in association with the neutral DM particle through the W boson, i.e. $pp \rightarrow W^* \rightarrow \eta^\pm \eta^0 \rightarrow \eta^0 \eta^0 W^{(*)}$ [55]. The inert doublet scalars can also be produced from their couplings to the SM Z boson via $pp \rightarrow \eta_R \eta_I j$ or the SM Higgs through $pp \rightarrow \eta^0 \eta^0 j$ (with j being an energetic jet) [56]. The inert-doublet sector can then be constrained by the mono- W [57, 58] and monojet [59, 60] searches at the LHC. Our model can in principle be distinguished from the pure scotogenic or pure type-II seesaw model at colliders using both inert-doublet and triplet-scalar signatures.

In the scotogenic model, the RHNs do not mix directly with the light active neutrinos. For our chosen BPs, the heavy RHNs are heavier than the inert-doublet and can only be produced at high-energy colliders from

the off-shell decay $\eta^{\pm*} \rightarrow \ell_\alpha N_i$, followed by $N_i \rightarrow \eta L_\alpha$. Due to the Majorana nature of the heavy RHNs, we can get same-sign dileptons, as in the Keung-Senjanović process [61], but now with missing transverse energy (MET) due to the presence of η^0 in the final state. The SM background for $\ell^\pm \ell^\pm + \text{MET}$ is expected to be higher than that without the MET, and a detailed simulation is needed to estimate the prospects of RHN signals in this model at future colliders.

Conclusion.— We have proposed a new technique to generate the observed baryon asymmetry of the universe via the tree-level interference of $2 \rightarrow 2$ scatterings. This is possible when we have at least two subprocesses in the $2 \rightarrow 2$ scatterings or $1 \rightarrow \mathcal{N}$ (with $\mathcal{N} \geq 3$) decays. The asymmetry comes from the absorptive part of the propagators. We have illustrated this mechanism explicitly in a well-motivated scotogenic model with type-II seesaw, in which the asymmetry is generated in the $\Delta L = 2$ processes $\eta\eta \rightarrow L_\alpha L_\beta$ mediated by s -channel triplets and t or u -channel RHNs. The neutrino masses receive contributions from both scotogenic and type-II seesaw mechanisms. The real part of the neutral component of the inert doublet η serves as a DM candidate. As shown in Fig. 3 the observed baryon asymmetry and DM relic density can be achieved for (sub)TeV inert-doublet and triplet masses.

Acknowledgments.— AD thanks the Particle Theory Group at Washington University in St. Louis for warm hospitality, where this work was initiated. YZ thanks Kaladi Babu for useful discussions, and the High Energy Theory Group at Oklahoma State University for warm hospitality, where this work was completed. The work of PSBD and YZ was supported in part by the U.S. Department of Energy under Grant No. DE-SC0017987 and in part by the MCSS. This work was also supported in part by the Neutrino Theory Network Program under Grant No. DE-AC02-07CH11359.

Appendix

Scalar masses.— All the scalar masses in the scotogenic plus type-II seesaw model with the SM Higgs H , the inert doublet η and the triplet Δ can be obtained from the scalar potential (9). When we take the first-order derivative of the potential with respect to the VEVs v and v_Δ , the solutions of the tadpole equations for $\{\mu_H^2, \mu_\Delta^2\}$ are given by

$$\mu_H^2 = \frac{1}{2}(\lambda_H v^2 - 2\sqrt{2}\mu_{H\Delta}v_\Delta + \lambda_{H\Delta}v_\Delta^2), \quad (19)$$

$$\mu_\Delta^2 = \frac{1}{2}(\lambda_\Delta v_\Delta^2 - 2\sqrt{2}\frac{\mu_{H\Delta}}{v_\Delta}v^2 + \lambda_{H\Delta}v^2). \quad (20)$$

After replacing $\{\mu_H^2, \mu_\Delta^2\}$ in the scalar potential, the mass

matrix for the real scalars reads

$$\mathcal{M}^0 = \begin{pmatrix} \lambda_H v^2 & -\sqrt{2}\mu_{H\Delta}v \\ -\sqrt{2}\mu_{H\Delta}v & \frac{\mu_{H\Delta}v^2}{\sqrt{2}v_\Delta} \end{pmatrix}, \quad (21)$$

from which we can get the two mass eigenvalues for the Higgs and scalar Δ_R^0 which is the real part of Δ^0 . In the case of $\mu_{H\Delta} \sim \mathcal{O}(100)$ keV, the two CP-even scalar masses turn out to be

$$m_h^2 \simeq \lambda_H v^2, \quad m_{\Delta_R^0}^2 \simeq \frac{\mu_{H\Delta}v^2}{\sqrt{2}v_\Delta}, \quad (22)$$

with the first one (h) identified as the SM-like Higgs boson. The masses of the pseudo-scalar and the charged scalars from the triplet are

$$m_{\Delta_I}^2 = \frac{\mu_{H\Delta}}{\sqrt{2}v_\Delta}(v^2 + 4v_\Delta^2), \quad (23)$$

$$m_{\Delta^\pm}^2 = m_{\Delta^{\pm\pm}}^2 = \left(\frac{\mu_{H\Delta}}{\sqrt{2}v_\Delta} + \frac{1}{4}\lambda'_{H\Delta} \right) (v^2 + 2v_\Delta^2). \quad (24)$$

Finally the masses for real scalar η_R , pseudo-scalar η_I and the charged scalars η^\pm from the Z_2 -odd doublet η are respectively

$$m_{\eta_{R,I}}^2 = \frac{1}{2} (2\mu_\eta^2 + (\lambda_{H\eta} + \lambda'_{H\eta} \pm \lambda''_{H\eta})v^2$$

$$+ (\lambda_{\eta\Delta}v_\Delta \mp 2\sqrt{2}\mu_{\eta\Delta})v_\Delta), \quad (25)$$

$$m_{\eta^\pm}^2 = \frac{1}{2} (2\mu_\eta^2 + \lambda_{H\eta}v^2 + (\lambda_{\eta\Delta} + \lambda'_{\eta\Delta})v_\Delta^2). \quad (26)$$

Thermal cross sections.— The general expression for the thermally averaged cross section for the processes in Eq. (17) is given by [44]

$$\begin{aligned} \langle \sigma v \rangle (i_1 i_2 \rightarrow f_1 f_2) &= \frac{1}{2T m_{i_1}^2 K_2(m_{i_1}/T) m_{i_2}^2 K_2(m_{i_2}/T)} \\ &\times \int_{s_{in}}^\infty \int_{-1}^1 \frac{1}{32\pi} \frac{|\mathcal{M}|^2}{\sqrt{s}} p_{i_1 i_2} p_{f_1 f_2} K_1(\sqrt{s}/T) ds d\cos\theta, \end{aligned} \quad (27)$$

where T is the temperature, K_i the modified Bessel functions of order i ,

$$p_{ij} \equiv \frac{1}{2} \sqrt{\frac{\lambda(s, m_i^2, m_j^2)}{s}}, \quad (28)$$

$$s_{in} \equiv \max[(m_{i_1} + m_{i_2})^2, (m_{f_1} + m_{f_2})^2], \quad (29)$$

$$\lambda(x, y, z) \equiv x^2 + y^2 + z^2 + 2xy + 2xz + 2yz, \quad (30)$$

\mathcal{M} is the amplitude for the process $i_1 i_2 \rightarrow f_1 f_2$. In Eq. (17) $\langle \sigma v \rangle_\delta(\eta\eta \rightarrow LL)$ is for the amplitude given in Eq. (15) which produces the lepton asymmetry. $\langle \sigma v \rangle_{\text{tot}}(\eta\eta \rightarrow LL)$ and $\langle \sigma v \rangle(\eta\bar{L} \rightarrow \eta L)$ are respectively for the amplitudes:

$$\begin{aligned} |\mathcal{M}^{\text{tot}}(\eta\eta \rightarrow LL)|^2 &= \frac{\hat{m}_\nu^2}{v_\Delta^2} \frac{F_I^2 \mu_{\eta\Delta}^2 s}{(s - m_\Delta^2)^2 + m_\Delta^2 \Gamma_\Delta^2} + \sum_i F_{II}^2 \frac{\hat{m}_\nu^2}{\Lambda_{ii}^2} m_{N_i}^2 s \left[\frac{1}{(t - m_{N_i}^2)} + \frac{1}{(u - m_{N_i}^2)} \right]^2 \\ &+ \frac{F_I F_{II} |\mu_{\eta\Delta}| (s - m_\Delta^2)}{(s - m_\Delta^2)^2 + m_\Delta^2 \Gamma_\Delta^2} \sum_i \frac{\hat{m}_\nu^2}{\Lambda_{ii} v_\Delta} m_{N_i} s \left[\frac{1}{(t - m_{N_i}^2)} + \frac{1}{(u - m_{N_i}^2)} \right], \end{aligned} \quad (31)$$

$$\begin{aligned} |\mathcal{M}(\eta\bar{L} \rightarrow \eta L)|^2 &= \frac{\hat{m}_\nu^2}{v_\Delta^2} \frac{F_I^2 \mu_{\eta\Delta}^2 (m_\eta^2 - t)}{(t - m_\Delta^2)^2} + \sum_i \frac{\hat{m}_\nu^2}{\Lambda_{ii}^2} \frac{F_{II}^2 m_{N_i}^2 s}{(s - m_{N_i}^2)^2 + m_{N_i}^2 \Gamma_{N_i}^2} \\ &+ \frac{F_I F_{II} |\mu_{\eta\Delta}| (m_\eta^2 - t)}{(t - m_\Delta^2)^2} \sum_i \frac{\hat{m}_\nu^2}{\Lambda_{ii} v_\Delta} m_{N_i} s \left[\frac{(s - m_{N_i}^2)}{(s - m_{N_i}^2)^2 + m_{N_i}^2 \Gamma_{N_i}^2} \right]. \end{aligned} \quad (32)$$

The cross section $\langle \sigma v \rangle(\eta\eta \rightarrow \text{SMSM})$ in Eq. (17) can be found in [36, 37], with “SM SM” referring to the all the possible channels involving the quarks, leptons, scalar and gauge bosons in the SM.

Benchmark points.— The three BPs used in our numerical analysis of the baryon asymmetry Y_{AB} and DM relic density $\Omega_{\text{DM}} h^2$ [cf. Fig. 3] are collected in Table I.

results. VI. Cosmological parameters,”

[arXiv:1807.06209](https://arxiv.org/abs/1807.06209) [[astro-ph.CO](https://arxiv.org/abs/1807.06209)].

- [2] A. D. Sakharov, “Violation of CP Invariance, C asymmetry, and baryon asymmetry of the universe,” *Pisma Zh. Eksp. Teor. Fiz.* **5** (1967) 32–35.
- [3] S. Dimopoulos and L. Susskind, “Baryon Asymmetry in the Very Early Universe,” *Phys. Lett.* **81B** (1979) 416–418.
- [4] S. Weinberg, “Cosmological Production of Baryons,” *Phys. Rev. Lett.* **42** (1979) 850–853.
- [5] M. Fukugita and T. Yanagida, “Baryogenesis Without Grand Unification,” *Phys. Lett.* **B174** (1986) 45–47.
- [6] J. M. Cline, “Baryogenesis,” in *Les Houches Summer*

[1] **Planck** Collaboration, N. Aghanim *et al.*, “Planck 2018

TABLE I. Three benchmark points for the numerical analysis presented in Fig. 3. All the quartic couplings in Eq. (9) not listed in this table are set to be zero. Here $\Delta m_{\eta^0} = m_{\eta_R} - m_{\eta_I}$ is the mass splitting between the two scalars η_R and η_I .

	BP1	BP2	BP3
v_Δ	1 keV	1 keV	1 keV
μ_η	600 GeV	1 TeV	1.5 TeV
$\mu_{H\Delta}$	33.6 keV	93.5 keV	210 keV
$\mu_{\eta\Delta}$	15i GeV	7.1i GeV	6i GeV
m_{N_1}	6 TeV	10 TeV	15 TeV
m_{N_2}	6.6 TeV	11 TeV	16.5 TeV
m_{N_3}	7.2 TeV	12 TeV	18 TeV
m_{η^0}	600 GeV	1 TeV	1.5 TeV
Δm_{η^0}	506 keV	300 keV	200 keV
m_{η^\pm}	606 GeV	1 TeV	1.5 TeV
m_{Δ^0}	1.2 TeV	2 TeV	3 TeV
m_{Δ^\pm}	1.2 TeV	2 TeV	3 TeV
$m_{\Delta^{\pm\pm}}$	1.6 TeV	2 TeV	3 TeV
λ_H	0.253	0.253	0.253
$\lambda_{H\eta}$	0.24	0.59	0.93
$\lambda'_{H\eta}$	-0.24	-0.59	-0.93
$\lambda''_{H\eta}$	1×10^{-5}	1×10^{-5}	1×10^{-5}

School - Session 86: Particle Physics and Cosmology: The Fabric of Spacetime Les Houches, France, July 31-August 25, 2006. [arXiv:hep-ph/0609145 \[hep-ph\]](#).

- [7] S. Davidson, E. Nardi, and Y. Nir, “Leptogenesis,” *Phys. Rept.* **466** (2008) 105–177, [arXiv:0802.2962 \[hep-ph\]](#).
- [8] D. V. Nanopoulos and S. Weinberg, “Mechanisms for Cosmological Baryon Production,” *Phys. Rev.* **D20** (1979) 2484.
- [9] R. Adhikari and R. Rangarajan, “Baryon number violation in particle decays,” *Phys. Rev.* **D65** (2002) 083504, [arXiv:hep-ph/0110387 \[hep-ph\]](#).
- [10] A. Bhattacharya, R. Gandhi, and S. Mukhopadhyay, “Revisiting the implications of CPT and unitarity for baryogenesis and leptogenesis,” *Phys. Rev.* **D89** no. 11, (2014) 116014, [arXiv:1109.1832 \[hep-ph\]](#).
- [11] M. Yoshimura, “Unified Gauge Theories and the Baryon Number of the Universe,” *Phys. Rev. Lett.* **41** (1978) 281–284. [Erratum: *Phys. Rev. Lett.* 42,746(1979)].
- [12] L. Bento and Z. Berezhiani, “Leptogenesis via collisions: The Lepton number leaking to the hidden sector,” *Phys. Rev. Lett.* **87** (2001) 231304, [arXiv:hep-ph/0107281](#).
- [13] I. Baldes, N. F. Bell, K. Petraki, and R. R. Volkas, “Particle-antiparticle asymmetries from annihilations,” *Phys. Rev. Lett.* **113** no. 18, (2014) 181601, [arXiv:1407.4566 \[hep-ph\]](#).
- [14] I. Baldes, N. F. Bell, A. Millar, K. Petraki, and R. R. Volkas, “The role of CP violating scatterings in baryogenesis - case study of the neutron portal,” *JCAP* **1411** no. 11, (2014) 041, [arXiv:1410.0108 \[hep-ph\]](#).
- [15] G. R. Farrar and G. Zaharijas, “Dark matter and the baryon asymmetry,” *Phys. Rev. Lett.* **96** (2006) 041302, [arXiv:hep-ph/0510079 \[hep-ph\]](#).
- [16] Y. Cui, L. Randall, and B. Shuve, “A WIMPY Baryogenesis Miracle,” *JHEP* **04** (2012) 075, [arXiv:1112.2704 \[hep-ph\]](#).
- [17] J. Kumar and P. Stengel, “WIMPY Leptogenesis With Absorptive Final State Interactions,” *Phys. Rev.* **D89** no. 5, (2014) 055016, [arXiv:1309.1145 \[hep-ph\]](#).
- [18] A. Dasgupta, C. Hati, S. Patra, and U. Sarkar, “A minimal model of TeV scale WIMPY leptogenesis,” [arXiv:1605.01292 \[hep-ph\]](#).
- [19] D. Borah, A. Dasgupta, and S. K. Kang, “Leptogenesis from Dark Matter Annihilations in Scotogenic Model,” [arXiv:1806.04689 \[hep-ph\]](#).
- [20] P. S. B. Dev, P. Di Bari, B. Garbrecht, S. Lavignac, P. Millington, and D. Teresi, “Flavor effects in leptogenesis,” *Int. J. Mod. Phys.* **A33** (2018) 1842001, [arXiv:1711.02861 \[hep-ph\]](#).
- [21] M. Drewes, B. Garbrecht, P. Hernandez, M. Kekic, J. Lopez-Pavon, J. Racker, N. Rius, J. Salvado, and D. Teresi, “ARS Leptogenesis,” *Int. J. Mod. Phys.* **A33** no. 05n06, (2018) 1842002, [arXiv:1711.02862 \[hep-ph\]](#).
- [22] A. Sirlin, “Theoretical considerations concerning the Z0 mass,” *Phys. Rev. Lett.* **67** (1991) 2127–2130.
- [23] P. A. Grassi, B. A. Kniehl, and A. Sirlin, “Width and partial widths of unstable particles,” *Phys. Rev. Lett.* **86** (2001) 389–392, [arXiv:hep-th/0005149 \[hep-th\]](#).
- [24] A. Pilaftsis and T. E. J. Underwood, “Resonant leptogenesis,” *Nucl. Phys.* **B692** (2004) 303–345, [arXiv:hep-ph/0309342 \[hep-ph\]](#).
- [25] P. S. B. Dev, M. Garny, J. Klaric, P. Millington, and D. Teresi, “Resonant enhancement in leptogenesis,” *Int. J. Mod. Phys.* **A33** (2018) 1842003, [arXiv:1711.02863 \[hep-ph\]](#).
- [26] E. Ma, “Verifiable radiative seesaw mechanism of neutrino mass and dark matter,” *Phys. Rev.* **D73** (2006) 077301, [arXiv:hep-ph/0601225 \[hep-ph\]](#).
- [27] M. Magg and C. Wetterich, “Neutrino Mass Problem and Gauge Hierarchy,” *Phys. Lett.* **94B** (1980) 61–64.
- [28] J. Schechter and J. W. F. Valle, “Neutrino Masses in SU(2) x U(1) Theories,” *Phys. Rev.* **D22** (1980) 2227.
- [29] T. P. Cheng and L.-F. Li, “Neutrino Masses, Mixings and Oscillations in SU(2) x U(1) Models of Electroweak Interactions,” *Phys. Rev.* **D22** (1980) 2860.
- [30] R. N. Mohapatra and G. Senjanovic, “Neutrino Masses and Mixings in Gauge Models with Spontaneous Parity Violation,” *Phys. Rev.* **D23** (1981) 165.
- [31] G. Lazarides, Q. Shafi, and C. Wetterich, “Proton Lifetime and Fermion Masses in an SO(10) Model,” *Nucl. Phys.* **B181** (1981) 287–300.
- [32] D. Borah, P. S. B. Dev, and A. Kumar, “TeV scale leptogenesis, inflaton dark matter and neutrino mass in a scotogenic model,” *Phys. Rev.* **D99** no. 5, (2019) 055012, [arXiv:1810.03645 \[hep-ph\]](#).
- [33] A. Merle and M. Platscher, “Running of radiative neutrino masses: the scotogenic model revisited,” *JHEP* **11** (2015) 148, [arXiv:1507.06314 \[hep-ph\]](#).
- [34] J. A. Casas and A. Ibarra, “Oscillating neutrinos and $\mu \rightarrow e\gamma$,” *Nucl. Phys.* **B618** (2001) 171–204, [arXiv:hep-ph/0103065 \[hep-ph\]](#).
- [35] M. D’Onofrio, K. Rummukainen, and A. Tranberg, “Sphaleron Rate in the Minimal Standard Model,” *Phys. Rev. Lett.* **113** no. 14, (2014) 141602, [arXiv:1404.3565 \[hep-ph\]](#).

- [36] R. Barbieri, L. J. Hall, and V. S. Rychkov, “Improved naturalness with a heavy Higgs: An Alternative road to LHC physics,” *Phys. Rev.* **D74** (2006) 015007, [arXiv:hep-ph/0603188 \[hep-ph\]](#).
- [37] L. Lopez Honorez, E. Nezri, J. F. Oliver, and M. H. G. Tytgat, “The Inert Doublet Model: An Archetype for Dark Matter,” *JCAP* **0702** (2007) 028, [arXiv:hep-ph/0612275 \[hep-ph\]](#).
- [38] J. A. Harvey and M. S. Turner, “Cosmological baryon and lepton number in the presence of electroweak fermion number violation,” *Phys. Rev.* **D42** (1990) 3344–3349.
- [39] V. A. Kuzmin, V. A. Rubakov, and M. E. Shaposhnikov, “On the Anomalous Electroweak Baryon Number Nonconservation in the Early Universe,” *Phys. Lett.* **155B** (1985) 36.
- [40] F. Staub, “SARAH 4 : A tool for (not only SUSY) model builders,” *Comput. Phys. Commun.* **185** (2014) 1773–1790, [arXiv:1309.7223 \[hep-ph\]](#).
- [41] **PandaX-II** Collaboration, X. Chen *et al.*, “Exploring the dark matter inelastic frontier with 79.6 days of PandaX-II data,” *Phys. Rev.* **D96** no. 10, (2017) 102007, [arXiv:1708.05825 \[hep-ex\]](#).
- [42] **XENON** Collaboration, E. Aprile *et al.*, “Search for WIMP Inelastic Scattering off Xenon Nuclei with XENON100,” *Phys. Rev.* **D96** no. 2, (2017) 022008, [arXiv:1705.05830 \[hep-ex\]](#).
- [43] **XMASS** Collaboration, T. Suzuki *et al.*, “Search for WIMP-¹²⁹Xe inelastic scattering with particle identification in XMASS-I,” *Astropart. Phys.* **110** (2019) 1–7, [arXiv:1809.05358 \[astro-ph.CO\]](#).
- [44] G. Bélanger, F. Boudjema, A. Goudelis, A. Pukhov, and B. Zaldivar, “micrOMEGAs5.0 : Freeze-in,” *Comput. Phys. Commun.* **231** (2018) 173–186, [arXiv:1801.03509 \[hep-ph\]](#).
- [45] **ATLAS** Collaboration, M. Aaboud *et al.*, “Search for doubly charged Higgs boson production in multi-lepton final states with the ATLAS detector using protonproton collisions at $\sqrt{s} = 13$ TeV,” *Eur. Phys. J.* **C78** no. 3, (2018) 199, [arXiv:1710.09748 \[hep-ex\]](#).
- [46] **CMS** Collaboration, “A search for doubly-charged Higgs boson production in three and four lepton final states at $\sqrt{s} = 13$ TeV,” Tech. Rep. CMS-PAS-HIG-16-036, CERN, Geneva, 2017. <http://cds.cern.ch/record/2242956>.
- [47] P. Fileviez Perez, T. Han, G.-y. Huang, T. Li, and K. Wang, “Neutrino Masses and the CERN LHC: Testing Type II Seesaw,” *Phys. Rev.* **D78** (2008) 015018, [arXiv:0805.3536 \[hep-ph\]](#).
- [48] A. Melfo, M. Nemevsek, F. Nesti, G. Senjanovic, and Y. Zhang, “Type II Seesaw at LHC: The Roadmap,” *Phys. Rev.* **D85** (2012) 055018, [arXiv:1108.4416 \[hep-ph\]](#).
- [49] M. Mitra, S. Niyogi, and M. Spannowsky, “Type-II Seesaw Model and Multilepton Signatures at Hadron Colliders,” *Phys. Rev.* **D95** no. 3, (2017) 035042, [arXiv:1611.09594 \[hep-ph\]](#).
- [50] P. S. B. Dev and Y. Zhang, “Displaced vertex signatures of doubly charged scalars in the type-II seesaw and its left-right extensions,” *JHEP* **10** (2018) 199, [arXiv:1808.00943 \[hep-ph\]](#).
- [51] S. Antusch, O. Fischer, A. Hammad, and C. Scherb, “Low scale type II seesaw: Present constraints and prospects for displaced vertex searches,” *JHEP* **02** (2019) 157, [arXiv:1811.03476 \[hep-ph\]](#).
- [52] Y. Du, A. Dunbrack, M. J. Ramsey-Musolf, and J.-H. Yu, “Type-II Seesaw Scalar Triplet Model at a 100 TeV pp Collider: Discovery and Higgs Portal Coupling Determination,” *JHEP* **01** (2019) 101, [arXiv:1810.09450 \[hep-ph\]](#).
- [53] P. Agrawal, M. Mitra, S. Niyogi, S. Shil, and M. Spannowsky, “Probing the Type-II Seesaw Mechanism through the Production of Higgs Bosons at a Lepton Collider,” *Phys. Rev.* **D98** no. 1, (2018) 015024, [arXiv:1803.00677 \[hep-ph\]](#).
- [54] P. S. B. Dev, M. J. Ramsey-Musolf, and Y. Zhang, “Doubly-Charged Scalars in the Type-II Seesaw Mechanism: Fundamental Symmetry Tests and High-Energy Searches,” *Phys. Rev.* **D98** no. 5, (2018) 055013, [arXiv:1806.08499 \[hep-ph\]](#).
- [55] N. Wan, N. Li, B. Zhang, H. Yang, M.-F. Zhao, M. Song, G. Li, and J.-Y. Guo, “Searches for Dark Matter via Mono-W Production in Inert Doublet Model at the LHC,” *Commun. Theor. Phys.* **69** no. 5, (2018) 617.
- [56] I. M. vila, V. De Romeri, L. Duarte, and J. W. F. Valle, “Minimalistic scotogenic scalar dark matter,” [arXiv:1910.08422 \[hep-ph\]](#).
- [57] **CMS** Collaboration, A. M. Sirunyan *et al.*, “Search for new physics in final states with an energetic jet or a hadronically decaying W or Z boson and transverse momentum imbalance at $\sqrt{s} = 13$ TeV,” *Phys. Rev.* **D97** no. 9, (2018) 092005, [arXiv:1712.02345 \[hep-ex\]](#).
- [58] **ATLAS** Collaboration, M. Aaboud *et al.*, “Search for dark matter in events with a hadronically decaying vector boson and missing transverse momentum in pp collisions at $\sqrt{s} = 13$ TeV with the ATLAS detector,” *JHEP* **10** (2018) 180, [arXiv:1807.11471 \[hep-ex\]](#).
- [59] **CMS** Collaboration, V. Khachatryan *et al.*, “Search for dark matter, extra dimensions, and unparticles in monojet events in protonproton collisions at $\sqrt{s} = 8$ TeV,” *Eur. Phys. J.* **C75** no. 5, (2015) 235, [arXiv:1408.3583 \[hep-ex\]](#).
- [60] **ATLAS** Collaboration, M. Aaboud *et al.*, “Search for dark matter and other new phenomena in events with an energetic jet and large missing transverse momentum using the ATLAS detector,” *JHEP* **01** (2018) 126, [arXiv:1711.03301 \[hep-ex\]](#).
- [61] W.-Y. Keung and G. Senjanovic, “Majorana Neutrinos and the Production of the Right-handed Charged Gauge Boson,” *Phys. Rev. Lett.* **50** (1983) 1427.